Heliyon

ELSEVIER

Reciprocal interactions between cancer and Schwann cells contribute to oral cancer progression and pain

Elizabeth Salvo [a], Prakaimuk Saraithong [a,1], Jared G. Curtin [b,2], Malvin N. Janal [c], Yi Ye [a,d,*]

[a] *Bluestone Center for Clinical Research, New York University College of Dentistry, New York, NY, 10010, USA*

[b] *DDS Program, New York University College of Dentistry, New York, NY, 10010, USA*

[c] *Epidemiology and Health Promotion, New York University College of Dentistry, New York, NY, 10010, USA*

[d] *Department of Oral and Maxillofacial Surgery, New York University College of Dentistry, New York, NY, 10010, USA*

[*] Corresponding author.

E-mail address: yy22@nyu.edu (Y. Ye).

[1] Current address: Department of Biologic and Materials Sciences, University of Michigan School of Dentistry, 1011 N. University Ave. Ann Arbor, MI 48109-1078, USA.

[2] Current address: Henry M. Goldman School of Dental Medicine, Oral and Maxillofacial Surgery Clinic, 4th floor, Boston University, 100 E Newton St, Boston, MA 02118, USA.

Abstract

Pain associated with oral squamous cell carcinoma (oral SCC) decreases quality of life and survival. The interaction between cancer and the peripheral nerves is known to initiate and amplify pain and contribute to carcinogenesis. Schwann cells envelop peripheral nerves and are activated in response to neuronal damage. The contributions of Schwann cells to oral SCC progression and pain are unknown. Using a non-contact co-culture model, we demonstrate that Schwann cells (RSC-96) and oral SCC cells (HSC-3) reciprocally interact to promote proliferation, migration, and invasion. Schwann cell-oral SCC interaction leads to increased production of adenosine, which stimulates cell proliferation and migration of both cell types. The adenosine receptor A2B (*ADORA2B*) is expressed on RSC-96 cells. We show that supernatant from the RSC-96 cells co-cultured with

HSC-3 cells induces increased mechanical hypersensitivity in mice compared to supernatant from control RSC-96 cells. Treatment with the ADORA2B antagonist PSB603 significantly inhibits co-culture interactions - proliferation and migration, and co-culture supernatant induced mechanical hypersensitivity. RSC-96 cells co-cultured with HSC-3 cells secrete increased amounts of the pronociceptive mediator, interleukin-6 (IL-6), which can be reduced by adding PSB603 into the co-culture. Our data support a reciprocal interaction between oral SCC and Schwann cells mediated by adenosine with potential to promote oral SCC progression and pain via increased secretion of IL-6.

Keywords: Neuroscience, Cancer research, Cell biology

1. Introduction

Oral squamous cell carcinoma (oral SCC) is painful and significantly impairs oral function and decreases quality of life in patients (Schmidt, 2014; Schmidt et al., 2010). Cancer pain is driven by the interaction between the cancer and peripheral nerves. Cancer releases algogenic mediators that excite and sensitize primary afferent neurons (Schmidt, 2014; Schmidt et al., 2010; Viet and Schmidt, 2010). Cancer invades and spreads along the nerve (*i.e.*, neural invasion, NI), leading to nerve injury and neuropathic pain (Mantyh, 2014; Yeh et al., 2016). Oral SCC pain could also be induced by pathological nerve sprouting into the tumor (Mantyh, 2014). However, current studies on oral SCC-nerve interaction focus only on the interaction between cancer and primary afferent neurons; the role of Schwann cells is overlooked.

Schwann cells are the most prevalent cell type in peripheral nerves, comprising 90% of the endoneurial space (Campana, 2007). Schwann cells are plastic; they become activated as evidenced by dedifferentiating, proliferating, and migrating in response to peripheral insults such as inflammation or nerve injury (Gosselin et al., 2010; Jessen et al., 2015; Scholz and Woolf, 2007; Ydens et al., 2013). They provide neuronal guidance and promote axonal growth during nerve regeneration and repair (Bhatheja and Field, 2006; Clements et al., 2017; Jessen et al., 2015). The process of nerve regeration in which Schwann cells play a critical role drives persistent neuropathic pain (Xie et al., 2017). Schwann cells are activated under hypoxic conditions and in the presence of pancreatic, colon, gastric and adenoid cystic carcinoma cells (Deborde et al., 2016; Demir et al., 2014, 2016). Activated Schwann cells promote cancer growth, invasion, dispersion, and secrete neurotrophic factors, chemokines/cytokines, proteases, and adhesion molecules (Bunimovich et al., 2017; Deborde et al., 2016; Deborde and Wong, 2017; Demir et al., 2014, 2017). Schwann cells recruit cancer cells to the nerve, and may promote neuronal sprouting into the cancer (Deborde et al., 2016; Deborde and Wong, 2017). Some neurotrophic factors and

pro-inflammatory cytokines released by activated Schwann cells could directly excite and sensitize primary afferent neurons (Gosselin et al., 2010; Ji et al., 2016; Scholz and Woolf, 2007). These findings suggest that Schwann cells could be activated by oral SCC and contribute to cancer progression and pain.

We showed previously that the oral SCC microenvironment contains high levels of adenosine 5′-triphosphate (ATP) in preclinical cancer models and human oral cancers (Ye et al., 2014b). ATP rapidly degrades to adenosine by two cell surface enzymes CD73 (*NT5E*) and CD39 (*ENTPD1*) (Di Virgilio and Adinolfi, 2017). Both CD73 and CD39 are upregulated in cancer, suggesting more rapid conversion of ATP to adenosine in the cancer microenvironment compared to normal conditions, resulting in adenosine accumulation (Di Virgilio and Adinolfi, 2017; Kazemi et al., 2017; Ohta, 2016). Adenosine is a neurotransmitter that regulates glial development, differentiation and glia-neuron communication (Stevens et al., 2002). The adenosine receptor A2B (*ADORA2B*) is overexpressed in oral SCC cell lines and human cancer specimens, and its expression levels significantly correlate with oral SCC growth (Kasama et al., 2015; Yamano et al., 2008). Adenosine is long-thought to be an inhibitory neurotransmitter for nociceptive signaling (Sawynok, 2016). However, recent studies show that sustained exposure to adenosine may underlie chronic pain by activating A2B receptors on circulating myeloid cells to release IL-6, which results in increased neuronal sensitivity and chronic pain (Hu et al., 2016).

In the present study we hypothesize a reciprocal interaction between oral SCC and Schwann cells that promotes cancer progression and pain. We propose that oral SCC and Schwann cell interact with each other through adenosine signaling and that interaction can be modulated by the adenosine receptor A2B. We will examine whether IL-6 is a Schwann cell derived nociceptive mediator that can be modulated by the A2B receptor.

2. Materials and methods

2.1. Cell culture and chemicals

Human oral SCC (HSC-3), human dysplastic oral keratinocytes (DOK), and rat Schwann cells (RSC-96) were purchased from ATCC. Cell passages between 4 and 10 were used for all experiments. Cells were grown in Dulbecco's Modified Eagle's Medium (DMEM) with 4.5 g/L glucose, L-glutamine and sodium pyruvate (Gibco, Thermo Fisher Scientific), supplemented with 10% fetal bovine serum (FBS), 100 μg/mL streptomycin sulfate, and 100 U/mL penicillin G at 37 °C in 5% CO_2. A highly selective A2B antagonist PSB603 (>17000-fold selectivity over other adenosine receptors) was obtained from Tocris Bioscience. Adenosine and adenosine 5′-triphosphate (ATP) were purchased from Sigma-Aldrich.

2.2. Animals

Six to eight week-old female BALB/cJ mice (Jackson laboratories) were housed in a temperature-controlled, pathogen free room on a 12:12 light/dark cycle (6 AM−6 PM) with *ad libitum* access to food and water. A total of 24 mice were used in the project. All procedures involving animals were approved by the New York University Institutional Animal Care and Use Committee (IACUC) under protocol # 160908-01, in accordance with the Guide for the Care and Use of Laboratory Animals published by the U.S. Institute for Laboratory Animal Research (8th edition). For all experiments, animals were habituated to handling prior to testing.

2.3. Schwann cell size measurement

To study the effect of oral SCC on Schwann cell morphology, 20×10^3 (20k) RSC-96 cells were cultured in 6-well plates with the same number of HSC-3 cells or DOK cells grown in cell inserts (3-µm pore size, Corning, Fig. 1A). Control RSC-96 cells were cultured with inserts containing just culture media DMEM. Following 24 hours in co-culture, cell inserts were discarded; RSC-96 cells were fixed and stained with Diff-Quik solution (Microptic) according the manufacturer's protocol. The RSC-96 cells were imaged under a Nikon Eclipse TI microscope. Cell body area was
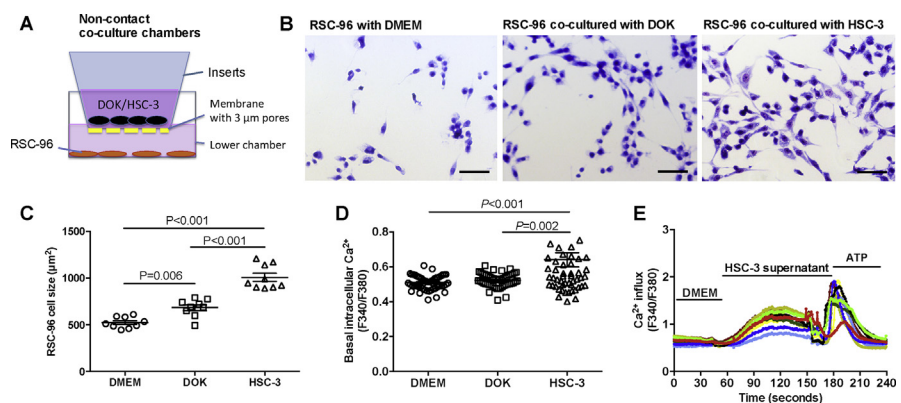
Fig. 1. Oral SCC induces Schwann cell hypertrophy and increased Ca^{2+} influx. (A) Co-culture model. To study Schwann cell morphology and basal intracellular Ca^{2+} levels following exposure to cancer cells, RSC-96 cells were cultured in the lower chamber, while either DOK or HSC-3 cells were cultured in the cell inserts. The inserts have 3 µm-sized pores that allow free exchange of media but do not allow cells to migrate through. (B) Representative images of RSC-96 cells cultured with inserts containing DMEM, DOK or HSC-3. Scale: 100 µm. (C) The mean size of RSC-96 cells was greater when co-cultured with HSC-3 cells, compared to RSC-96 cells co-culture with DOK or with DMEM alone. (D) Intracellular Ca^{2+} concentration was higher in Schwann cells co-cultured with HSC-3 cells compared with co-culture with DOK or with DMEM alone. (E) Representative Ca^{2+} responses of RSC-96 cells to DMEM, HSC-3 supernatant, and 100 µM ATP. Each color represents a different cell. One-way ANOVA with Tukey's post hoc analysis.

automatically measured using Nikon Element software. Three images were taken for each well, and at least three wells were used for each treatment.

2.4. Ca^{2+} imaging

Cultured RSC-96 cells were loaded with 1 μM Fura-2 AM (Molecular Probes) for 30 minutes and washed with HBSS. Fluorescence was detected by a Nikon Eclipse TI microscope fitted with a 20X fluor/NA 0.75 objective lens. Fluorescence images of 340 and 380 excitation wavelengths were collected and analyzed with the Nikon TI Element Software. To study the effect of cancer cells on Schwann cell intracellular Ca^{2+} levels, RSC-96 cells were seeded onto glass coverslips and co-cultured with either inserts (3-μm pore size, Corning) containing DMEM alone, inserts with DOK culture, or inserts with HSC-3 culture (Fig. 1A). After 24 hours of co-culture, the inserts were removed, RSC-96 cells were perfused with HBSS, and alternating fluorescent images at 340nm and 380nm wavelength were taken for one minute. The 340/380 ratios in one-minute were averaged and compared among control RSC-96 cells, RSC-96 cells co-cultured with DOK cells, and RSC-96 cells co-cultured with HSC-3 cells. To study whether cancer cells induce Ca^{2+} influx in normal RSC-96 cells, HSC-3 cell supernatant was collected using a published method (Scheff et al., 2017; Ye et al., 2011, 2014a, 2014b, 2018). HSC-3 cells were cultured until 90% confluence. Media were replaced with fresh serum free media 48 hours prior to collection of supernatant. Ca^{2+} imaging was conducted on RSC-96 cells by applying DMEM for one minute, followed by HSC-3 cell supernatant for two minutes, and 100 μM of ATP (a positive control) for another 1 minute. Cells were counted as HSC-3 supernatant responsive if the 340/380 ratio is ≥ 0.2 from baseline according to a published method (Ye et al., 2014b).

2.5. Cell growth measurement with a real time cell analyzer (RTCA)

The real time growth kinetics of RSC-96 cells and HSC-3 cells were examined using the Real-Time Cell Analyzer (RTCA) (xCELLigence System, Roche Applied Science) according to published methods (Roshan Moniri et al., 2015). After background recordings, 10k cells were added to each well of the plate. Cell growth was monitored for 18 hours to enter their logarithmic growth phase, before 100 μL control culture media, drug treatment, or cell inserts were added (Fig. 2A). For co-culture experiments (Fig. 2A, Fig. 3A), either HSC-3 (10k or 20k) or RSC-96 (10k or 20k) cells were placed into cell inserts (3-μm pore size, xCELLigence Systems). Cell impedance was recorded for an additional 48−72 hours. Cell growth rate (slope, delta cell index/over delta time) was calculated based on the most linear portion of the cell growth curve before the plateau, using the RTCA Software Package 1.2. At least 5 wells were used for each treatment.
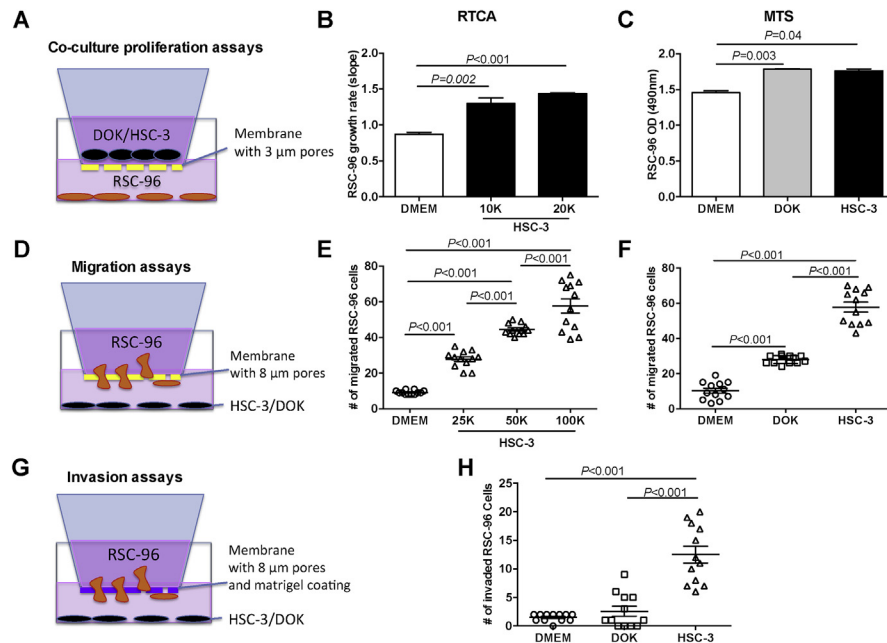
Fig. 2. Oral SCC promotes Schwann cell proliferation, migration, and invasion. (A) To study the effect of HSC-3 or DOK cells on Schwann cell proliferation, RSC-96 cells were cultured in the lower chamber, while either DOK or HSC-3 cells were cultured in the cell inserts. (B) Growth rate of RSC-96 cells measured by the RTCA, increased with HSC-3 cell number. (C) Optical density (OD) measured using the MTS assay increased when RSC-96 cells were co-cultured with DOK or HSC-3 cells compared to DMEM alone. Kruskal-Wallis with Dunn's test. (D) To study the effect of HSC-3 or DOK cells on RSC-96 migration, RSC-96 cells were cultured in a migration chamber. Either HSC-3 or DOK cells were seeded in the bottom chamber. (E) Migration of RSC-96 cells towards HSC-3 cells increased in a cell number dependent manner. (F) Increased numbers of RSC-96 cells migrated toward HSC-3 cells compared to DOK or DMEM. (G) To study effect of HSC-3 or DOK cells on RSC-96 invasion, RSC-96 cells were cultured in invasion chambers. Either HSC-3 or DOK cells were seeded in the bottom chamber. (H) Increased numbers of invaded RSC-96 cells towards HSC-3 compared to DOK or DMEM. One-way ANOVA with Tukey's post hoc analysis.

2.6. Cell proliferation assay

Cell growth was further confirmed with CellTiter 96® Aqueous One Solution Reagent (Promega) following the manufacturer's instructions. Either HSC-3 or RSC-96 cells were seeded at a density of 10k cells/well in 96-well plates. After 24 hours in culture, cell inserts for 96-well plates (3-μm pore size, xCELLigence Systems) or drugs were added into each well. Cells were incubated for another 48 hours until cell proliferation was measured at 490 nm optical density (OD) using a microplate reader (Promega). For co-culture experiments, the same density of HSC-3 (10k) and RSC-96 (10k) cells was used (Fig. 2A, Fig. 3A). Experiments were performed in triplicates and were repeated twice.

2.7. Migration and invasion assays

Cell migration assays were performed using 6-well culture plates and transwell Boyden chambers with an 8-μm pore size according to the manufacturer's instructions
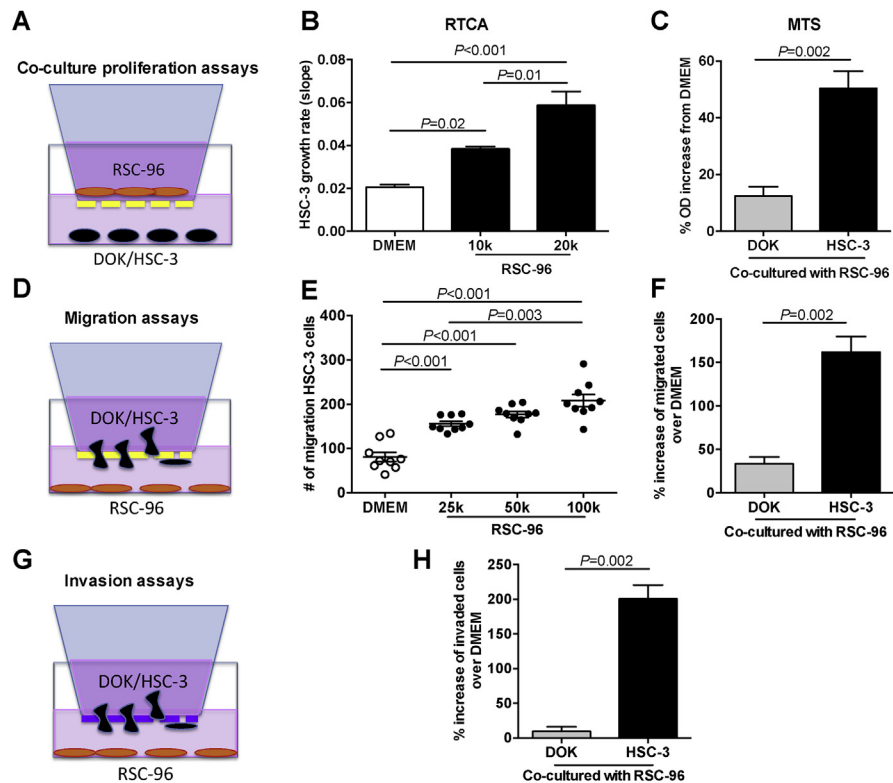
Fig. 3. Schwann cells promote oral SCC proliferation, migration, and invasion. (A) To study the effect of RSC-96 cells on proliferation, HSC-3 or DOK cells were cultured in the lower chamber, and RSC-96 cells were cultured in the cell inserts. Cell culture media DMEM in the lower chamber was used as control. (B) Growth rate of HSC-3 cells, measured with the RTCA, increased with RSC-96 cell number. (C) HSC-3 cells proliferated more than DOK when co-cultured with RSC-96 cells. Data are presented as a percentage increase in OD from DMEM treated controls. (D) To study the effect of RSC-96 on cancer cell migration, HSC-3 or DOK cells were cultured in migration chambers with RSC-96 cells or DMEM (control) in the bottom chamber. (E) HSC-3 cells migrated towards RSC-96 cells in a cell number dependent manner. (F) HSC-3 cells migrated more than DOK towards RSC-96 cells. Data are presented as a percentage increase in number of migrated cells towards RSC-96 relative to DMEM controls. (G) To study effect of RSC-96 cells on cancer cell invasion, HSC-3 and DOK cells were cultured in invasion chambers with RSC-96 cells seeded at the bottom chamber. Bottom chambers containing DMEM alone were used as controls. (H) Increased invasion of HSC-3 cells compared to DOK cells in the presence of RSC-96 cells. Data are presented as percentage increase in number of invaded cells towards RSC-96 relative to DMEM treated controls. B, E, one-way ANOVA with Tukey's post hoc analysis; C, Mann-Whitney U-test, F, H, student's t-test.

(Corning, Fig. 2D, Fig. 3D). For the invasion assays we used 6-well culture plates and matrigel coated Boyden chambers with 8-µm pore size (BD Biosciences, Fig. 2G, Fig. 3G). To examine the migration of RSC-96 cells towards HSC-3 cells, 10k RSC-96 cells were seeded on the migration chambers; 25k, 50k or 100k HSC-3 cells were seeded in the bottom chamber. Similarly, to examine the migration of HSC-3 cells towards RSC-96 cells, 10k HSC-3 cells were seeded on the upper migration chambers. Lower chambers contained 25k, 50k, or 100k RSC-96 cells.

All cells were cultured in DMEM plus 1% FBS. Lower chambers with DMEM plus 1% FBS without cells were used as controls. To compare the effect of DOK and HSC-3 cells on RSC-96 cell migration and invasion, or the effect of RSC-96 cells on DOK and HSC-3 cell migration and invasion, 100k cells were seeded in the bottom chambers and 10k cells were seeded on the upper migration chambers. After 24 hours incubation, the Boyden chambers were removed, non-migrating cells were removed, and membranes containing migrated or invaded cells were fixed and stained with Diff-Quik solution (Microptic) according the manufacturer's protocol. The number of migrated or invaded cells on the lower side of the membrane was counted under a Nikon Eclipse TI microscope. Four photomicrographs per membrane were randomly taken and quantified for data analysis. Experiments were performed in triplicates.

2.8. ATP and adenosine quantification

To measure the ATP and the adenosine production in both HSC-3 and RSC-96 cells, HSC-3 and RSC-96 cells (100k each) were co-cultured in a 6-well plate with cell culture inserts. Inserts containing DMEM were used as controls. Triplicate wells were used for each treatment. Forty-eight hours following co-culture, when the cells were confluent, the inserts were removed. Either HSC-3 or RSC-96 cells in the culture plate were washed twice with PBS. Cells were collected in RIPA buffer (Thermo Fisher Scientific) with 10% protease inhibitor cocktail (Thermo Fisher Scientific). Cell lysates were centrifuged at 13,000g for 10 min at 4 °C. ATP concentration in RSC-96 and HSC-3 cell lysates was determined using ENLITEN ATP assay kit (Promega). Luminescence intensity was determined using a luminometer (Promega). Adenosine concentration in RSC-96 and HSC-3 cell lysates was measured using a fluorometric adenosine assay kit (BioVision) following the manufacturer's instructions. The fluorescent intensity of adenosine was measured using a SpectraMax M5 plate reader (Molecular Devices). All samples were run in duplicate.

2.9. Real-time PCR

Total RNA was isolated from RSC-96 cells using the Qiagen AllPrep DNA/RNA Micro Kit (Qiagen Inc.). Reverse transcription was carried out with Quantitect Reverse Transcription Kit (Qiagen Inc.) according to the manufacturer's instructions. Quantitative real-time PCR was performed with the Taqman Gene Expression Assay Kit (Applied Biosystems Inc.). The housekeeping gene β-actin was used as the internal control gene. Primers were purchased from Life Technologies (rat A2B: RN00567697_m1; rat IL-6: RN01410330_m1; rat β-actin: Rn00667869_m1). Relative quantification analysis of gene expression data was calculated using the $2^{-\Delta\Delta Ct}$ method.

2.10. Western blot

For A2B protein quantification, RSC-96 cells were co-cultured with DOK cells or HSC3 cells for 48 hours before harvest. Cells were lysed and homogenized in ice-cold RIPA buffer (Thermo Fisher Scientific) with 10% protease inhibitor cocktail (Thermo Fisher Scientific). Homogenates were centrifuged at 13,000g for 10 min at 4 °C. The supernatant was collected and stored at -80 °C. Protein concentration of the homogenates was determined using the bicinchoninic acid (BCA) protein assay kit (Thermo Fisher Scientific). For western blot analysis, 30 μg of protein extract was fractionated on a 12% Mini-Protean TGX gel (Bio-Rad) and transferred onto nitrocellulose membranes (Thermo Fisher Scientific). Membranes were blocked for 1 hour with 5% bovine serum albumin (BSA) in PBS containing 0.1% Tween-20, and then incubated overnight at 4 °C at a 1:1000 dilution with rabbit anti-adenosine A2B receptor (Chemicon, AB1589P) or rabbit anti-GAPDH antibody (Cell Signaling, 2118). Secondary antibody HRP-conjugated goat anti-rabbit IgG (Santa Cruz Biotechnology, sc-2030) was used at 1:5000 dilution. The signal was detected by Clarity Western ECL Substrate (Bio-Rad) and analyzed using ChemiDoc MP Imaging System with Image Lab Software (Bio-Rad).

2.11. Immunofluorescent staining

RSC-96 cells were grown overnight at 37 °C on 12-mm glass cover slips coated with 100 μg/mL Poly-L-ornithine (Sigma-Aldrich) and 6 μg/mL of laminin (Sigma-Aldrich). Control RSC-96 cells were cultured with inserts containing DMEM. Treated RSC-96 cells were co-cultured with the same ratio of HSC-3 cells in cell inserts containing DMEM. For A2B antagonist treatment, PSB603 was added into the co-culture to a final concentration of 10 μM. After 48 hours, cells were washed twice with PBS, fixed in ice-cold methanol for 5 min at room temperature, and permeabilized with 0.2% Triton X-100 for 5 min. Cells were incubated with Superblock (Thermo Fisher Scientific) for 1 hour before addition of primary antibodies, rabbit anti-adenosine A2B receptor (1:200, Chemicon, AB1589P) or mouse anti-rat-IL-6 (1:100, Abcam, AB9324) at 4 °C overnight. The primary antibodies were validated with western blot. After 3 washes with PBS, the coverslips were incubated with goat anti-rabbit Alexa Fluor 488 (1:500) or rabbit anti-mouse Texas Red (1:1000, Abcam AB6726) in PBS for 1 hour at room temperature. The specificity of the secondary antibodies was previously tested without applying primary antibodies. Cover slips were washed and mounted on slides in aqueous mounting medium with DAPI to stain the Nuclei (Santa Cruz) and imaged with a Nikon Eclipse TI microscope. Three images were taken for each coverslip. Fluorescence intensity of each image was quantified using Nikon Element Software. Experiments were run in triplicate.

2.12. Supernatant collection and pain behavior assessment

To determine whether Schwann cells co-cultured with cancer cells can directly trigger a nociceptive response, we injected supernatant from control (DMEM) RSC-96 cells and RSC-96 cells co-cultured with HSC-3 cells into the mouse hind paw and measured paw withdrawal thresholds. RSC-96 cell supernatant was prepared using a non-contact co-culture approach. 100k RSC-96 cells were seeded onto a 6-well culture plate. Cell culture inserts containing DMEM alone (control), or 100k HSC-3 cells (treatment) were then placed on top of the RSC-96 culture. To prevent the contamination of release products from HSC-3 cells, two days following co-culture, cell inserts containing either DMEM or HSC-3 were discarded and RSC-96 growth media was replaced by 1 mL serum-free DMEM. Control RSC-96 cells or RSC-96 cells co-cultured with HSC-3 cells were allowed to grow for another 48 hours before supernatant was collected and centrifuged to remove cell debris. 50 μL of fresh prepared supernatant was injected to the mid-plantar region of the mouse right hind paw under anesthesia with isoflurane. Six mice received control RSC-96 supernatant; 6 mice received supernatant from RSC-96 cells co-cultured with HSC-3 cells.

To determine whether modulation of the Schwann cell-cancer interaction alters cancer-associated nociception, we mixed equal numbers (2×10^6) of HSC3 cells and RSC-96 cells in 10-cm cell culture dishes with DMEM supplemented with 10% FBS. 16 hours later the old media was removed and cells were washed with clear DMEM to remove unattached cells. Vehicle treatment plates receive 3 mL of clear serum-free DMEM containing 3 μL of DMSO (vehicle control). Drug treated plates received 3 μL PSB603 stock dissolved in DMSO into 3 mL of clear serum-free DMEM (1 μM final concentration). Cells were treated for 24 hours before the supernatant was collected and centrifuged briefly to remove cell debris. 50 μL of fresh prepared supernatant was injected to the mid-plantar region of the mouse right hind paw under anesthesia with isoflurane. 6 mice received vehicle supernatant from the co-culture of RSC-96 and HSC-3 cells, and another 6 mice received supernatant from A2B antagonist PSB603 treated co-culture.

For the paw withdrawal assay, mice were allowed to acclimate to the behavior room, the experimenter, and the measuring device for 2 weeks before a baseline paw withdrawal threshold was taken. Supernatant-injected mice were placed individually in a plastic cage with a wire mesh floor. One hour was allowed for recovery from anesthesia and acclimation before testing. The mid-plantar right hind paw was stimulated with a series of von Frey fibers with logarithmically incremental stiffness (TouchTest®, North Coast Medical Inc.) using the up-and-down methods (Chaplan et al., 1994). The von Frey fibers were held perpendicular to the testing surface with sufficient force to cause buckling. A positive

response was considered if the paw was sharply withdrawn and if there was an immediate flinching upon removal of fiber. The fibers were presented at least 5 seconds apart to allow resolution of previous stimuli. Paw withdrawal thresholds were taken at every hour for three hours after injection. Three to six repetitive trials were averaged as the threshold for each mouse at different time points. Animals were randomly assigned into groups. The number of animals per group was determined based on our previous publications on behavioral measurement following HSC-3 supernatant injection (Lam and Schmidt, 2010; Ye et al., 2014b, 2018). The experimenter who performed the behavior testing was blinded to treatment groups.

2.13. Statistical analysis

GraphPad *Prism 6.0* was used to perform the statistical analysis. Data were checked for normal distributions using D'Agostino & Pearson omnibus normality test. Student's t-test or Mann-Whitney U test was used to compare two groups depending on data normality. One-way Analysis of Variance (ANOVA) with a Tukey's test or Kruskal-Wallis with Dunn's test was used to compare multiple groups. The behavioral responses to mechanical stimuli over time among groups were tested using two-way repeated ANOVA, followed by Sidak's post hoc test. The significance levels were set at $P < 0.05$, $P < 0.01$, or $P < 0.001$. Results were presented as mean $\pm$ standard error of the mean (SEM).

3. Results

3.1. Oral SCC cells induce hypertrophy and Ca^{2+} accumulation in Schwann cells

RSC-96 cells co-cultured with HSC-3 cells exhibited increased cytoplasmic area compared to control RSC-96 cells ($P < 0.001$, HSC-3 vs. DMEM, Fig. 1B−C) or RSC-96 cells co-cultured with non-tumorigenic DOK cells ($P < 0.001$, HSC-3 vs. DOK, Fig. 1B−C). Since Ca^{2+} signaling regulates Schwann cell function and excitability (Nedergaard et al., 2010), we examined whether HSC-3 cells induce Ca^{2+} accumulation within RSC-96 cells. Intracellular Ca^{2+} concentration, as measured by the 340/380 ratio, was higher in RSC-96 cells co-cultured with HSC-3, compared with RSC-96 co-cultured with DOK or RSC-96 grown in DMEM alone (N = 52 per treatment, $P < 0.001$, HSC-3 vs. DMEM, and $P = 0.002$, HSC-3 vs. DOK co-culture, Fig. 1D). We also observed a slowly increased Ca^{2+} influx in RSC-96 cells (180 HSC-3 supernatant responsive cells in 250 ATP responsive cells; 72%) when perfused with HSC-3 cell supernatant compared to DMEM, while ATP induced a sharp Ca^{2+} increase in these cells (Fig. 1E).

3.2. Schwann cells are more proliferative, migratory, and invasive in the presence of oral SCC cells

Growth rate of RSC-96 cells increased when co-cultured with either 10k or 20k HSC-3 cells compared to DMEM alone as measured with the RTCA assay ($P =$ 0.002, 10k HSC-3 vs. DMEM, $P < 0.001$, 20k HSC-3 vs. DMEM, Fig. 2B). Proliferation of RSC-96 cells, as measured by the CellTiter 96® proliferation assay, increased when co-cultured with DOK or HSC-3 cells compared to DMEM alone (P=0.003, DOK vs. DMEM, $P = 0.04$, HSC-3 vs. DMEM, Fig. 2C). RSC-96 cells migrated toward HSC-3 cells in a cell number dependent manner (Fig. 2E) with greater migration of RSC-96 cells when co-cultured with HSC-3 compared to DOK or DMEM ($P < 0.001$; Fig. 2F). By contrast, whereas increased proliferation and migration of RSC-96 cells were observed in the presence of both HSC-3 and DOK cells, only HSC-3 cells induced increased invasion of RSC-96 cells through matrigel ($P < 0.001$, HSC-3 compared to DOK cells and DMEM, respectively; Fig. 2H).

3.3. Oral SCC cells are more proliferative, migratory, and invasive in the presence of Schwann cells

The growth rate of HSC-3 cells increased when co-cultured with either 10k or 20k RSC-96 cells compared to DMEM alone (P=0.02, 10k RSC-96 vs. DMEM, $P =$ 0.01, 10k RSC-96 vs. 20k RSC-96, $P < 0.001$, 20k RSC-96 vs. DMEM, Fig. 3B). Similarly, migration of HSC-3 cells increased in a cell number dependent manner when co-cultured with RSC-96 cells (Fig. 3E). Compared to DOK cells, HSC-3 cells were more proliferative ($P = 0.002$, Fig. 3C), migratory ($P = 0.002$, Fig. 3F) and invasive ($P = 0.002$, Fig. 3H) in the presence of RSC-96 cells.

3.4. Schwann cell and oral SCC cell Co-culture leads to increased adenosine production

We next investigated whether Schwann cells and oral SCC cells change their ATP and adenosine production when co-cultured together. We detected increased adenosine concentration in the cell lysate of HSC-3 cells co-cultured with RSC-96 (178 μM ± 4.36), compared to DMEM control (129 μM ± 5.7; Fig. 4A; $P = 0.002$), while the ATP concentration in HSC-3 cell lysate (14.29 μM ± 1.27) was not different when co-cultured with RSC-96 cells compared to the media control (15 μM ± 1.74, $P = 0.51$). Adenosine concentration in the cell lysate of RSC-96 cells also increased following co-culture with HSC-3 cells (248 μM ± 19.42), compared to the DMEM control (193 μM ± 48.45; $P = 0.02$). The ATP concentration in cell lysate was significantly lower in RSC-96 cells following co-culture with HSC-3 cells (0.10 μM ± 0.13) compared to the DMEM control (2.90 μM ± 0.76, $P = 0.002$, Fig. 4B).
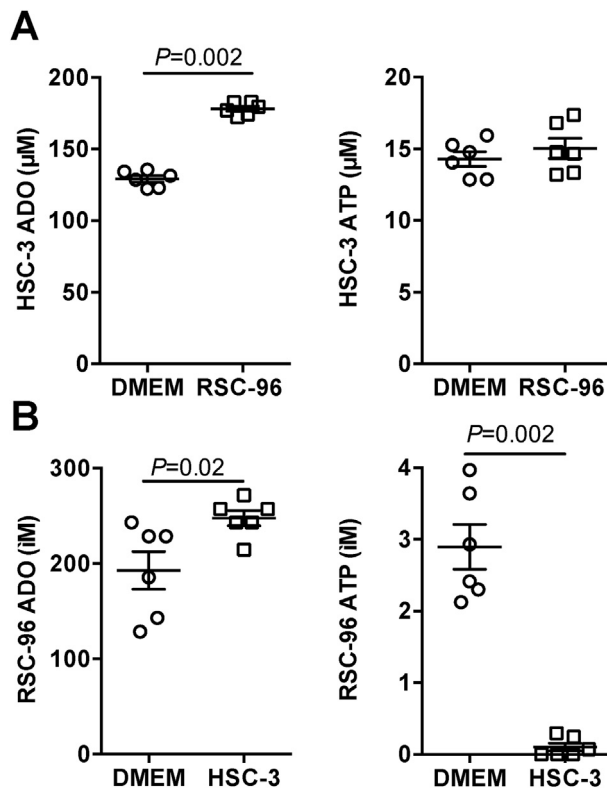
Fig. 4. Schwann cell and oral SCC interaction leads to increased adenosine production from both cell types. (A) Adenosine (ADO) concentration increases in HSC-3 cell lysate following co-culture with RSC-96 cells compared to the DMEM control. ATP concentration in HSC-3 cell lysate does not change following co-culture with RSC-96 cells compared to the DMEM control. (B) The ADO concentration in the cell lysate of RSC-96 cells increases following co-culture with HSC-3 cells compared to the DMEM control. The ATP concentration in RSC-96 cell lysate is significantly lower following co-culture with HSC-3 cells compared to the DMEM control. Mann-Whitney U-test.

3.5. Adenosine and the A2B receptor mediate Schwann cell proliferation and migration

To determine whether the observed changes in proliferation and migration of RSC-96 cells following co-culture with HSC-3 cells were mediated by adenosine and the A2B receptor, we first determined that the adenosine receptor A2B was expressed by RSC-96 cells although receptor expression levels were not altered by co-culture (Fig. 5A−D). Addition of 1 µM adenosine in DMEM increased RSC-96 cell proliferation and migration compared to the DMEM control ($P < 0.001$ and $P = 0.02$, respectively, Fig. 6A−B) and the increase was inhibited in a dose dependent manner by addition of the A2B antagonist PSB603 (Fig. 6A−B). Similarly, increased proliferation and migration of RSC-96 cells was observed when the cells were co-cultured with HSC-3 cells, and the increase was reversed by addition of the A2B antagonist PSB603 into the HSC-3 culture (Fig. 6C−D).
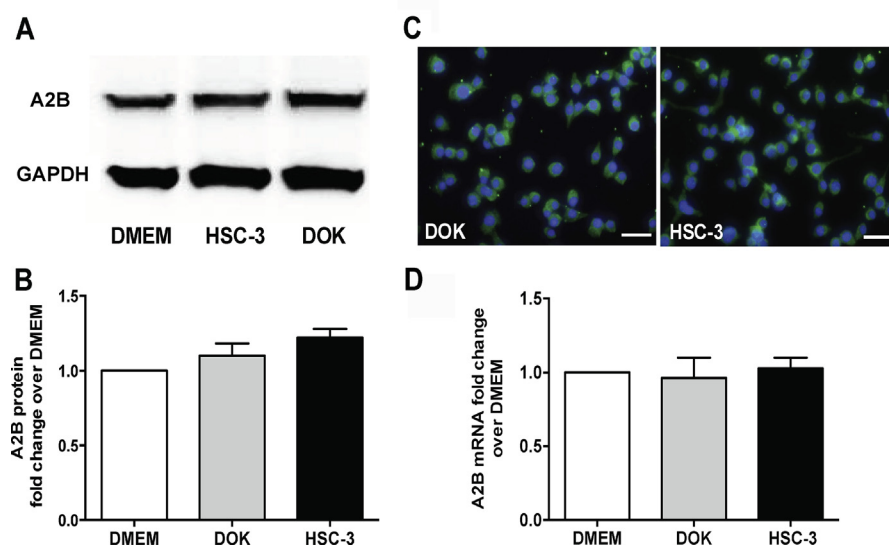
Fig. 5. A2B receptors are expressed in Schwann cells. (A) Western blot image of A2B expression in RSC-96 cells. GAPDH is used as a housekeeping control. Relative expression of A2B protein in RSC-96 cells co-cultured with DOK or HSC-3 is presented as fold change over DMEM treated RSC-96 cells. (B) Western blot quantification of A2B protein expression in RSC-96 cells. (C) Immunofluorescence labeling of the A2B receptor (green) and nucleus (DAPI, blue) in RSC-96 cells co-cultured with either DOK or HSC-3. Scale: 100 μm. (D) Relative A2B mRNA fold change in RSC-96 cells co-cultured with either DOK or HSC-3 over control RSC-96 cells. No differences are detected across different groups. Kruskal-Wallis test followed by Dunn's multiple comparison analysis.

3.6. Adenosine and the A2B receptor mediate oral SCC cell proliferation and migration

Addition of 1 μM of adenosine in DMEM increased HSC-3 cell growth rate ($P <$ 0.001, Fig. 7A) and migration ($P < 0.001$, Fig. 7B) compared to the DMEM control, and the increased proliferation and migration induced by adenosine were inhibited by the A2B antagonist PSB603 in a dose dependent manner (Fig. 7A−B). In the co-culture model, RSC-96 induced increased proliferation ($P < 0.001$) of HSC-3 cells; adding the A2B antagonist PSB603 into the HSC-3 culture significantly reduced HSC-3 cell growth ($P < 0.001$, Fig. 7C). Adding the A2B antagonist PSB603 into the co-culture significantly reduced HSC-3 cell migration towards RSC-96 in a concentration dependent manner ($P < 0.001$, 1 μM PSB603+RSC-96 vs. RSC-96, $P = 0.04$, 1 μM PSB603+RSC-96 vs. 100 nM PSB603+RSC-96, $P = 0.08$, 100 nM PSB603+RSC-96 vs. RSC-96 Fig. 7D).

3.7. Schwann cells and the A2B receptor modulate oral SCC-induced nociception

We previously showed that HSC-3 supernatant induced mechanical hypersensitivity when injected into mice (Scheff et al., 2017; Ye et al., 2014b). To determine whether
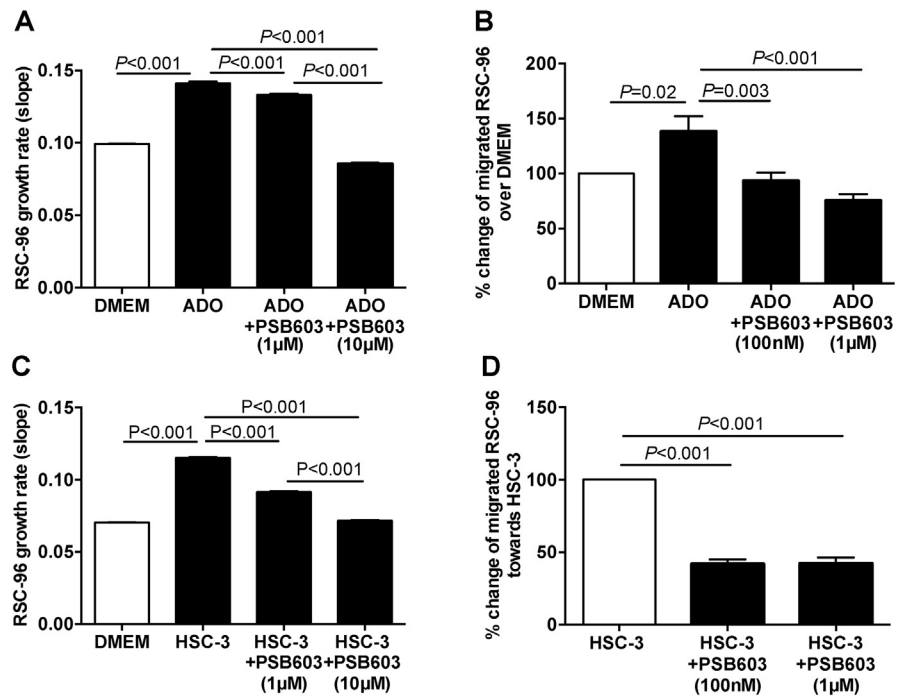
Fig. 6. The adenosine A2B receptor mediates adenosine-induced Schwann cell proliferation and migration. (A) Adenosine (1 μM) increases the growth rate of RSC-96 cells compared to the DMEM control measured by the RTCA. The A2B antagonist PSB603 (either at 1 μM or 10 μM) inhibits adenosine induced increase in RSC-96 growth. (B) Migration of Schwann cells is increased when adenosine (1 μM) is added to the media at the bottom chamber compared to the DMEM control. The A2B antagonist PSB603 added to the RSC-96 culture (either at 100 nM or 1 μM) inhibits adenosine induced increase in RSC-96 cell migration. (C) Increased RSC-96 proliferation in the presence of HSC-3 cells is inhibited by treating RSC-96 with either 1 μM or 10 μM PSB603. (D) RSC-96 migration towards HSC-3 cells are inhibited by treating of RSC-96 culture with 1 μM PSB603. One-way ANOVA with Tukey's post hoc analysis.

Schwann cells contribute to cancer pain, RSC-96 cells were co-cultured with HSC-3 cells for two days to induce Schwann cell activation. The cell culture inserts containing HSC-3 cells were discarded, fresh media was added, and the RSC-96 cells were cultured alone for two days before the supernatant was collected. Control RSC-96 cells were cultured in the same condition with inserts filled with DMEM in the absence of HSC-3 cells. Supernatant from control RSC-96 cells alone decreased mechanical thresholds from baseline in mice ($P < 0.001$) and the decrease was augmented with supernatant from RSC-96 cells co-cultured with HSC-3 cells at two hours following injection ($P = 0.03$, Fig. 8A). No difference was detected between the two groups three hours following injection ($P = 0.06$). To examine whether HSC-3 and RSC-96 cell interaction induces nociceptive behavior in mice, and whether the A2B receptor antagonist can inhibit the resulted nociceptive behaviors, we injected supernatant from the HSC-3 and RSC-96 mixed co-culture with and without PSB603 treatment. The supernatant from the co-culture mix induced a decrease in mechanical thresholds from pre-injection baseline, lasted for at least
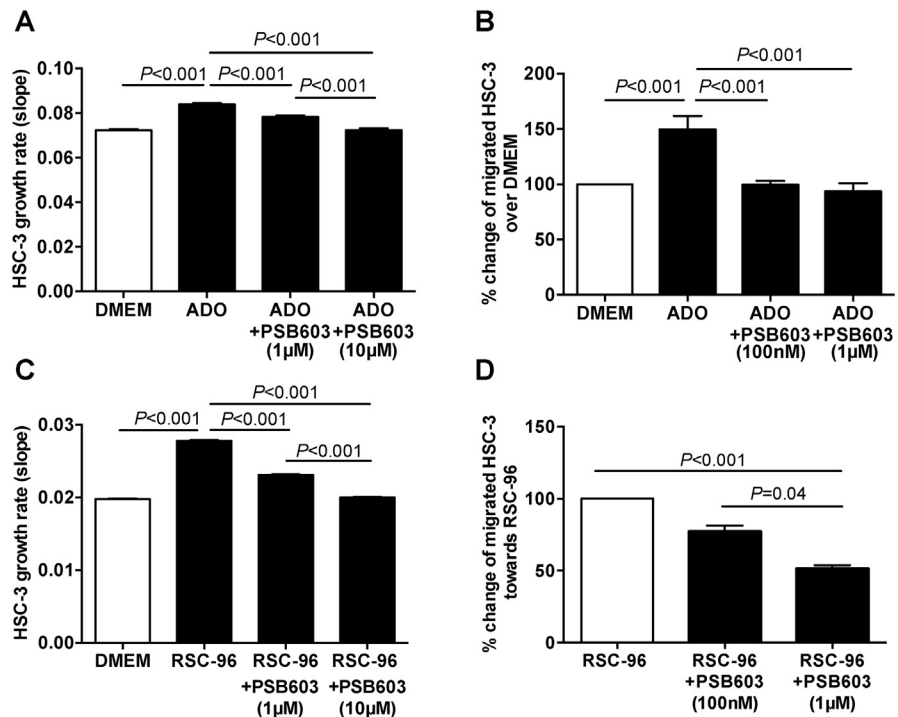
Fig. 7. The adenosine A2B receptor mediates adenosine-induced Schwann cell proliferation and migration. (A) ADO (1 μM) increases the growth rate of HSC-3 cells compared to the DMEM control measured by the RTCA. The A2B antagonist PSB603 (either at 1 μM or 10 μM) inhibits adenosine induced increase in HSC-3 cell growth. (B) Migration of HSC-3 cells is increased when adenosine (1 μM) was added to the media at the bottom chamber compared to the DMEM control. The A2B antagonist PSB603 (either at 100 nM or 1 μM) added to the HSC-3 culture inhibits adenosine-induced increase in HSC-3 cell migration. (C) Increased HSC-3 cell proliferation in the presence of RSC-96 cells is inhibited by treating HSC-3 cells with either 1 μM or 10 μM PSB603. (D) HSC-3 cell migration towards RSC-96 cells is inhibited by treatment of HSC-3 cell culture with 1 μM PSB603. One-way ANOVA with Tukey's post hoc analysis.

three hours ($P < 0.001$, Fig. 8B). Supernatant from the PSB603-treated co-culture significantly increased mechanical thresholds in mice compared to the control supernatant (Fig. 8B).

Since the A2B receptor has been shown to modulate the expression of IL-6 (Merighi et al., 2017), a nociceptive mediator, we investigated the effect of HSC-3 cells and the A2B antagonist on IL-6 mRNA and protein expression in RSC-96 cells. In non-contact co-culture with HSC-3 cells, IL-6 mRNA expression increased in RSC-96 cells compared to the DMEM control ($P < 0.001$, Fig. 8C), and this increase was inhibited by addition of PSB603 to the cell co-culture media ($P = 0.002$, Fig. 8C). Expression of IL-6 protein in RSC-96 cells was also increased following co-culture with HSC-3 cells in inserts compared to the DMEM control ($P < 0.001$, Fig. 8D−E), and this increase was inhibited by PSB603 treatment in the cell co-culture media ($P = 0.009$, Fig. 8D−E).
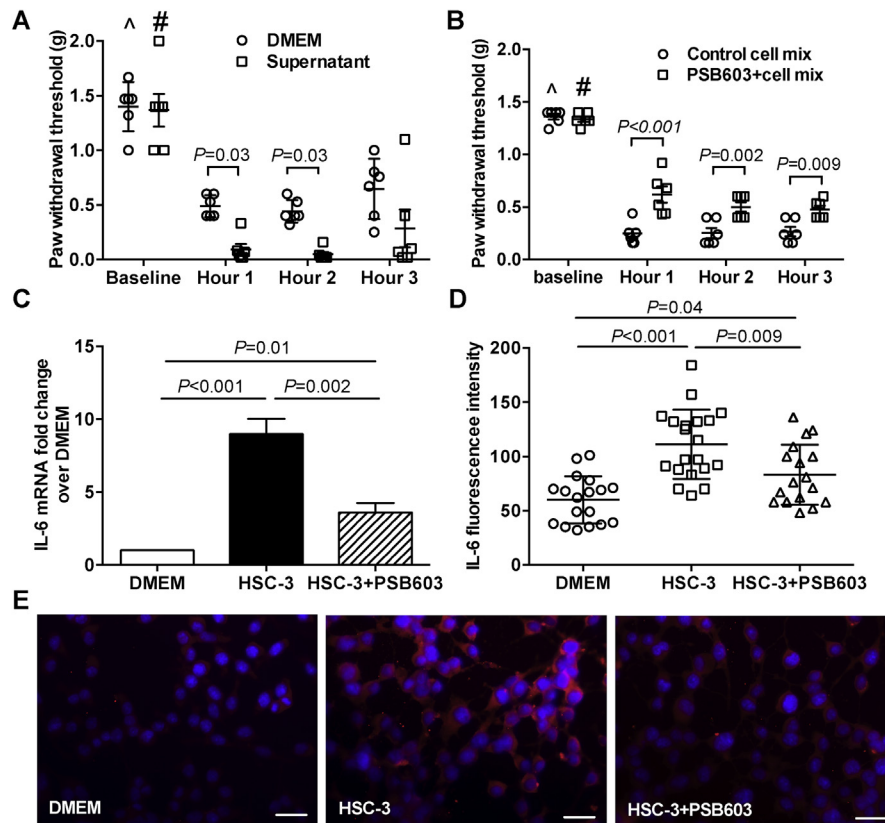
Fig. 8. Schwann cells and the adenosine receptor A2B modulate oral SCC-induced nociception. (A) Paw withdrawal thresholds of mice before and at 1 hour, 2 hours, 3 hours following injection with supernatant from control RSC-96 (DMEM) or supernatant from RSC-96 cells co-cultured with HSC-3 cells. Time factor: $F_{(3,30)} = 67.46$, $P < 0.001$; Group factor: $F_{(1,10)} = 11.94$, $P = 0.006$. (B) Paw withdrawal thresholds of mice before and at 1 hour, 2 hours, 3 hours following injection of supernatant from mixed RSC-96 and HSC-3 co-culture, or supernatant from mixed RSC-96 and HSC-3 co-culture treated with PSB603 (1 μM). Time factor: $F_{(3,30)} = 244.5$, $P < 0.001$; Group factor: $F_{(1,10)} = 28.67$, $P < 0.001$. (C) IL-6 mRNA expression fold change over DMEM in RSC-96 cells co-cultured with HSC-3, or PSB603 (10 μM) treated RSC-96 cells co-cultured with HSC-3. (D) IL-6 fluorescence intensity in control RSC-96 cells, or RSC-96 cells co-cultured with HSC-3, or RSC-96 cells co-cultured with HSC-3 plus PSB603 treatment. (E) Photomicrograph examples of control RSC-96 cells, RSC-96 cells co-cultured with HSC-3, and RSC-96 cells co-cultured with HSC-3 plus PSB603 treatment. Scale bar = 100 μm. A-B, Two-way repeated ANOVA with Sadik's test. ˆ, $P < 0.001$, baseline vs. other time points in the control group. #, $P < 0.001$, baseline vs. other time points in the treatment group. N = 6 per group. C-D, One-way ANOVA with Tukey's post hoc analysis.

4. Discussion

Here we investigated a bidirectional interaction between Schwann cells and oral SCC. Our study demonstrates that oral SCC activates Schwann cells. Oral SCC-induced activation of Schwann cells is characterized by cell body enlargement, increased migration and proliferation; these features are similar to the Schwann cell response to nerve injury (Scholz and Woolf, 2007). We also show that Schwann cells facilitate oral SCC proliferation, migration, and invasion *in vitro*. Using a

supernatant paw injection model, we demonstrate that oral SCC activated Schwann cells could induce nociceptive behaviors in mice.

Emerging evidence suggests a cancer-promoting role of Schwann cells. Consistent with our own findings, increased cancer migration and invasion induced by Schwann cells has been reported in pancreatic, prostate, and colon cancer studies (Deborde et al., 2016; Deborde and Wong, 2017; Sroka et al., 2016). Schwann cells induce cancer spread and protrusion formation (Deborde et al., 2016), and epithelial-mesenchymal transition (EMT)(Fujii-Nishimura et al., 2018; Shan et al., 2016). Furthermore, Schwann cells contribute to increased nerve innervation (*i.e.*, hyperin-nervation) commonly seen in cancer (Deborde and Wong, 2017) because of their known function in inducing nerve branching, arborization, and outgrowth (Armati and Mathey, 2013; Jessen et al., 2008; Kidd et al., 2013). Schwann cells are not only present within the axon, but are also present around neurites or nerve terminals (Kidd et al., 2013), where they can make direct contact with cancer cells and help recruit cancer cells to the nerve (Deborde and Wong, 2017). Removal of Schwann cells following chemical or surgical ablations of nerves might explain decreased tumor growth and progression in animal models of prostate, gastric, and pancreatic cancers (Magnon et al., 2013; Saloman et al., 2016; Zhao et al., 2014). Additionally, Schwann cells might contribute to cancer progression by initiating the process of neural invasion (Azam and Pecot, 2016). Schwann cells migrate towards pancreatic cancer cells before cancer migrate towards Schwann cells; and the presence of Schwann cells in pancreatic precancer sites is associated with increased frequency of neural invasion in malignant pancreatic cancers (Demir et al., 2014).

Our data suggest that the Schwann cell-oral SCC interaction is mediated by adenosine and its receptor A2B. Growing evidence indicates that adenosine and receptor A2B potentially play a pathophysiological role in human cancer and might serve as novel therapy for cancer (Kazemi et al., 2017). Receptor A2B in the tumor, fibroblasts, endothelial and immune cells increase cancer progression through immunosuppressive activity, tumor angiogenesis, proliferation, and metastasis (Kasama et al., 2015; Kazemi et al., 2017; Kumar, 2013; Ohta, 2016). Our findings affirm that A2B activation favors cancer progression. We did not observe an upregulation of A2B receptors on Schwann cells co-cultured with oral SCC, suggesting that activation of A2B receptors alone is sufficient to mediate cell proliferation and migration. Activated A2B receptors have the ability to couple to either a G_q protein or a G_s subtype of $G\alpha$ proteins to mediate different cellular functions (Fernandez-Gallardo et al., 2016; Schulte and Fredholm, 2003). A2B receptor activation has been shown to increase both mRNA and protein levels of IL-6, PLC, PKC-ε, PKC-δ and p38 signaling, while inhibition of A2B receptor activation pharmacologically by the antagonist PSB603 was associated with a reduction in p38 phosphorylation and IL-6 secretion in microglial cells (Merighi et al., 2017). Future studies are

needed to pinpoint the downstream signaling pathway upon A2B activation in Schwann cells in the presence of oral SCC.

Our data show that Schwann cells co-cultured with oral SCC induce increased mechanical hypersensitivity in mice and IL-6 is one of the possible nociceptive mediators released by oral SCC activated Schwann cells. Schwann cells co-cultured with oral SCC released more IL-6 compared to control Schwann cells; the A2B receptor antagonist reduced IL-6 release from Schwann cells co-cultured with oral SCC. In parallel, the A2B receptor antagonist inhibited the nociceptive behavior induced by Schwann cells co-cultured with oral SCC. Adenosine can be either pronociceptive or analgesic depending on the type of receptor and cells it acts upon and the duration of its action (Hu et al., 2016; Sawynok, 2016). Adenosine is known to trigger IL-6 release in many cell types and the A2B receptor modulates IL-6 production (Merighi et al., 2017; Wei et al., 2013). Our findings are further supported by a recent study showing mice lacking an enzyme that breaks down adenosine had increased chronic pain (Hu et al., 2016). Accumulated adenosine activates A2B receptors in myeloid cells and leads to an increase in circulating IL-6 and soluble IL-6 receptor, which causes STAT3 phosphorylation and TRPV1 expression in primary afferent neurons (Hu et al., 2016). In pancreatic cancer, however, Schwann cell activation and increased IL-6 are negatively correlated with cancer pain (Demir et al., 2016, 2017). The authors found greater abundance of Schwann cells in premalignant pancreatic intraepithelial neoplasia (not painful) compared to the painful pancreatic adenomas (Demir et al., 2014, 2016). The authors suggest that pancreatic precancer is not painful due to IL-6 produced by activated Schwann cells, which blocks glial activation in the central nervous system (Demir et al., 2016). However, the authors also report increased secretion of other known nociceptive mediators such as TNF-α, CCL2, IL-8 by activated Schwann cells (Demir et al., 2016). IL-6 activates glial cells and causes nociceptive behaviors in many animal models (Dubovy et al., 2010; Ellis and Bennett, 2013; Hu et al., 2016; Moini-Zanjani et al., 2016; Scholz and Woolf, 2007; Serizawa et al., 2018; Ye et al., 2011; Zhang and An, 2007). Similar to pancreatic precancer, patients with oral dysplasia usually do not report pain, while pain is a prominent feature accompanying oral SCC, especially oral SCC with NI (Lam and Schmidt, 2011; Yeh et al., 2016). Our data show that Schwann cells are activated more when exposed to oral SCC cells compared to oral precancer cells. While additional studies are needed to confirm the role of Schwann cell derived IL-6 in oral SCC induced pain, activated Schwann cells could release other nociceptive mediators such as NGF and TNF-α - two commonly reported Schwann cell mediators (Ji et al., 2016; Scholz and Woolf, 2007). In addition, Schwann cells may indirectly induce increased cancer pain through promoting cancer growth and migration, which could lead to accumulation of cancer-derived pain mediators (Scheff et al., 2017; Schmidt et al., 2007, 2010; Ye et al., 2011) proximal to the nerve terminals and axons.

5. Conclusions

The present study demonstrated a role of Schwann cells in cancer progression and pain in an oral SCC model. Oral SCC cells and Schwann cells exhibited a mutual affinity and growth advantage, mediated by adenosine and the A2B receptor. Proliferating cancer cells and Schwann cells lead to the secretion of nociceptive mediators such as IL-6 in the cancer microenvironment, which could trigger and amplify cancer pain.

Declarations

Author contribution statement

Elizabeth Salvo, Yi Ye: Conceived and designed the experiments; Performed the experiments; Analyzed and interpreted the data; Wrote the paper.

Prakaimuk Saraithong: Performed the experiments; Analyzed and interpreted the data.

Jared Curtin: Performed the experiments.

Malvin Janal: Analyzed and interpreted the data.

Funding statement

Competing interest statement

The authors declare no conflict of interest.

Additional information

Supplementary content related to this article has been published online at https://doi.org/10.1016/j.heliyon.2019.e01223.

Acknowledgements

References

Armati, P.J., Mathey, E.K., 2013. An update on Schwann cell biology–immunomodulation, neural regulation and other surprises. J. Neurol. Sci. 333, 68–72.

Azam, S.H., Pecot, C.V., 2016. Cancer's got nerve: Schwann cells drive perineural invasion. J. Clin. Invest. 126, 1242−1244.

Bhatheja, K., Field, J., 2006. Schwann cells: origins and role in axonal maintenance and regeneration. Int. J. Biochem. Cell Biol. 38, 1995−1999.

Bunimovich, Y.L., Keskinov, A.A., Shurin, G.V., Shurin, M.R., 2017. Schwann cells: a new player in the tumor microenvironment. Cancer Immunol. Immunother. 66, 959−968.

Campana, W.M., 2007. Schwann cells: activated peripheral glia and their role in neuropathic pain. Brain Behav. Immun. 21, 522−527.

Chaplan, S.R., Bach, F.W., Pogrel, J.W., Chung, J.M., Yaksh, T.L., 1994. Quantitative assessment of tactile allodynia in the rat paw. J. Neurosci. Methods 53, 55−63.

Clements, M.P., Byrne, E., Camarillo Guerrero, L.F., Cattin, A.L., Zakka, L., Ashraf, A., Burden, J.J., Khadayate, S., Lloyd, A.C., Marguerat, S., Parrinello, S., 2017. The wound microenvironment reprograms Schwann cells to invasive mesenchymal-like cells to drive peripheral nerve regeneration. Neuron 96, 98−114.

Deborde, S., Omelchenko, T., Lyubchik, A., Zhou, Y., He, S., McNamara, W.F., Chernichenko, N., Lee, S.-Y., Barajas, F., Chen, C.-H., Bakst, R.L., Vakiani, E., He, S., Hall, A., Wong, R.J., 2016. Schwann cells induce cancer cell dispersion and invasion. J. Clin. Invest. 126, 1538−1554.

Deborde, S., Wong, R.J., 2017. How Schwann cells facilitate cancer progression in nerves. Cell. Mol. Life Sci. CMLS.

Demir, I.E., Boldis, A., Pfitzinger, P.L., Teller, S., Brunner, E., Klose, N., Kehl, T., Maak, M., Lesina, M., Laschinger, M., Janssen, K.-P., Algül, H., Friess, H., Ceyhan, G.O., 2014. Investigation of Schwann cells at neoplastic cell sites before the onset of cancer invasion. JNCI J. Natl. Cancer Inst. 106 dju184-dju184.

Demir, I.E., Kujundzic, K., Pfitzinger, P.L., Saricaoglu, O.C., Teller, S., Kehl, T., Reyes, C.M., Ertl, L.S., Miao, Z., Schall, T.J., Tieftrunk, E., Haller, B., Diakopoulos, K.N., Kurkowski, M.U., Lesina, M., Kruger, A., Algul, H., Friess, H., Ceyhan, G.O., 2017. Early pancreatic cancer lesions suppress pain through CXCL12-mediated chemoattraction of Schwann cells. Proc. Natl. Acad. Sci. U. S. A 114, E85−E94.

Demir, I.E., Tieftrunk, E., Schorn, S., Saricaoglu, O.C., Pfitzinger, P.L., Teller, S., Wang, K., Waldbaur, C., Kurkowski, M.U., Wormann, S.M., Shaw, V.E., Kehl, T., Laschinger, M., Costello, E., Algul, H., Friess, H., Ceyhan, G.O., 2016. Activated

Schwann cells in pancreatic cancer are linked to analgesia via suppression of spinal astroglia and microglia. Gut 65, 1001−1014.

Di Virgilio, F., Adinolfi, E., 2017. Extracellular purines, purinergic receptors and tumor growth. Oncogene 36, 293−303.

Dubovy, P., Klusakova, I., Svizenska, I., Brazda, V., 2010. Satellite glial cells express IL-6 and corresponding signal-transducing receptors in the dorsal root ganglia of rat neuropathic pain model. Neuron Glia Biol. 6, 73−83.

Ellis, A., Bennett, D.L., 2013. Neuroinflammation and the generation of neuropathic pain. Br. J. Anaesth. 111, 26−37.

Fernandez-Gallardo, M., Gonzalez-Ramirez, R., Sandoval, A., Felix, R., Monjaraz, E., 2016. Adenosine Stimulate Proliferation and Migration in Triple Negative Breast Cancer Cells. PLoS One 11, e0167445.

Fujii-Nishimura, Y., Yamazaki, K., Masugi, Y., Douguchi, J., Kurebayashi, Y., Kubota, N., Ojima, H., Kitago, M., Shinoda, M., Hashiguchi, A., Sakamoto, M., 2018. Mesenchymal-epithelial transition of pancreatic cancer cells at perineural invasion sites is induced by Schwann cells. Pathol. Int. 68, 214−223.

Gosselin, R.D., Suter, M.R., Ji, R.R., Decosterd, I., 2010. Glial cells and chronic pain. Neuroscientist 16, 519−531.

Hu, X., Adebiyi, M.G., Luo, J., Sun, K., Le, T.T., Zhang, Y., Wu, H., Zhao, S., Karmouty-Quintana, H., Liu, H., Huang, A., Wen, Y.E., Zaika, O.L., Mamenko, M., Pochynyuk, O.M., Kellems, R.E., Eltzschig, H.K., Blackburn, M.R., Walters, E.T., Huang, D., Hu, H., Xia, Y., 2016. Sustained elevated adenosine via ADORA2B promotes chronic pain through neuro-immune interaction. Cell Rep. 16, 106−119.

Jessen, K.R., Mirsky, R., Lloyd, A.C., 2015. Schwann cells: development and role in nerve repair. Cold Spring. Harb. Perspect. Biol. 7, a020487.

Jessen, K.R., Mirsky, R., Salzer, J., 2008. Introduction. Schwann cell biology. Glia 56, 1479−1480.

Ji, R.R., Chamessian, A., Zhang, Y.Q., 2016. Pain regulation by non-neuronal cells and inflammation. Science 354, 572−577.

Kasama, H., Sakamoto, Y., Kasamatsu, A., Okamoto, A., Koyama, T., Minakawa, Y., Ogawara, K., Yokoe, H., Shiiba, M., Tanzawa, H., Uzawa, K., 2015. Adenosine A2b receptor promotes progression of human oral cancer. BMC Canc. 15, 563.

Kazemi, M.H., Raoofi Mohseni, S., Hojjat-Farsangi, M., Anvari, E., Ghalamfarsa, G., Mohammadi, H., Jadidi-Niaragh, F., 2017. Adenosine and adenosine receptors in the immunopathogenesis and treatment of cancer. J. Cell. Physiol. n/a−n/a.

Kidd, G.J., Ohno, N., Trapp, B.D., 2013. Biology of Schwann cells. Handb. Clin. Neurol. 115, 55−79.

Kumar, V., 2013. Adenosine as an endogenous immunoregulator in cancer pathogenesis: where to go? Purinergic Signal. 9, 145−165.

Lam, D.K., Schmidt, B.L., 2010. Serine proteases and protease-activated receptor 2-dependent allodynia: a novel cancer pain pathway. Pain 149, 263−272.

Lam, D.K., Schmidt, B.L., 2011. Orofacial pain onset predicts transition to head and neck cancer. Pain 152, 1206−1209.

Magnon, C., Hall, S.J., Lin, J., Xue, X., Gerber, L., Freedland, S.J., Frenette, P.S., 2013. Autonomic nerve development contributes to prostate cancer progression. Science 341, 1236361.

Mantyh, P.W., 2014. Bone cancer pain: from mechanism to therapy. Curr. Opin. Support. Palliat. Care 8, 83−90.

Merighi, S., Bencivenni, S., Vincenzi, F., Varani, K., Borea, P.A., Gessi, S., 2017. A2B adenosine receptors stimulate IL-6 production in primary murine microglia through p38 MAPK kinase pathway. Pharmacol. Res. 117, 9−19.

Moini-Zanjani, T., Ostad, S.N., Labibi, F., Ameli, H., Mosaffa, N., Sabetkasaei, M., 2016. Minocycline effects on IL-6 concentration in macrophage and microglial cells in a rat model of neuropathic pain. Iran. Biomed. J. 20, 273−279.

Nedergaard, M., Rodriguez, J.J., Verkhratsky, A., 2010. Glial calcium and diseases of the nervous system. Cell Calcium 47, 140−149.

Ohta, A., 2016. A metabolic immune checkpoint: adenosine in tumor microenvironment. Front. Immunol. 7, 109.

Roshan Moniri, M., Young, A., Reinheimer, K., Rayat, J., Dai, L.J., Warnock, G.L., 2015. Dynamic assessment of cell viability, proliferation and migration using real time cell analyzer system (RTCA). Cytotechnology 67, 379−386.

Saloman, J.L., Albers, K.M., Li, D., Hartman, D.J., Crawford, H.C., Muha, E.A., Rhim, A.D., Davis, B.M., 2016. Ablation of sensory neurons in a genetic model of pancreatic ductal adenocarcinoma slows initiation and progression of cancer. Proc. Natl. Acad. Sci. U. S. A 113, 3078−3083.

Sawynok, J., 2016. Adenosine receptor targets for pain. Neuroscience 338, 1−18.

Scheff, N.N., Ye, Y., Bhattacharya, A., MacRae, J., Hickman, D.N., Sharma, A.K., Dolan, J.C., Schmidt, B.L., 2017. Tumor necrosis factor alpha secreted from oral squamous cell carcinoma contributes to cancer pain and associated inflammation. Pain 158, 2396−2409.

Schmidt, B.L., 2014. The neurobiology of cancer pain. Neuroscientist 20, 546−562.

Schmidt, B.L., Hamamoto, D.T., Simone, D.A., Wilcox, G.L., 2010. Mechanism of cancer pain. Mol. Interv. 10, 164−178.

Schmidt, B.L., Pickering, V., Liu, S., Quang, P., Dolan, J., Connelly, S.T., Jordan, R.C., 2007. Peripheral endothelin A receptor antagonism attenuates carcinoma-induced pain. Eur. J. Pain 11, 406−414.

Scholz, J., Woolf, C.J., 2007. The neuropathic pain triad: neurons, immune cells and glia. Nat. Neurosci. 10, 1361−1368.

Schulte, G., Fredholm, B.B., 2003. The G(s)-coupled adenosine A(2B) receptor recruits divergent pathways to regulate ERK1/2 and p38. Exp. Cell Res. 290, 168−176.

Serizawa, K., Tomizawa-Shinohara, H., Magi, M., Yogo, K., Matsumoto, Y., 2018. Anti-IL-6 receptor antibody improves pain symptoms in mice with experimental autoimmune encephalomyelitis. J. Neuroimmunol. 319, 71−79.

Shan, C., Wei, J., Hou, R., Wu, B., Yang, Z., Wang, L., Lei, D., Yang, X., 2016. Schwann cells promote EMT and the Schwann-like differentiation of salivary adenoid cystic carcinoma cells via the BDNF/TrkB axis. Oncol. Rep. 35, 427−435.

Sroka, I.C., Chopra, H., Das, L., Gard, J.M., Nagle, R.B., Cress, A.E., 2016. Schwann cells increase prostate and pancreatic tumor cell invasion using laminin binding A6 integrin. J. Cell. Biochem. 117, 491−499.

Stevens, B., Porta, S., Haak, L.L., Gallo, V., Fields, R.D., 2002. Adenosine: a neuron-glial transmitter promoting myelination in the CNS in response to action potentials. Neuron 36, 855−868.

Viet, C.T., Schmidt, B.L., 2010. Understanding oral cancer in the genome era. Head Neck 32, 1246−1268.

Wei, W., Du, C., Lv, J., Zhao, G., Li, Z., Wu, Z., Hasko, G., Xie, X., 2013. Blocking A2B adenosine receptor alleviates pathogenesis of experimental autoimmune encephalomyelitis via inhibition of IL-6 production and Th17 differentiation. J. Immunol. 190, 138−146.

Xie, W., Strong, J.A., Zhang, J.M., 2017. Active nerve regeneration with failed target reinnervation drives persistent neuropathic pain. eNeuro 4.

Yamano, Y., Uzawa, K., Shinozuka, K., Fushimi, K., Ishigami, T., Nomura, H., Ogawara, K., Shiiba, M., Yokoe, H., Tanzawa, H., 2008. Hyaluronan-mediated motility: a target in oral squamous cell carcinoma. Int. J. Oncol. 32.

Ydens, E., Lornet, G., Smits, V., Goethals, S., Timmerman, V., Janssens, S., 2013. The neuroinflammatory role of Schwann cells in disease. Neurobiol. Dis. 55, 95−103.

Ye, Y., Bae, S.S., Viet, C.T., Troob, S., Bernabe, D., Schmidt, B.L., 2014a. IB4(+) and TRPV1(+) sensory neurons mediate pain but not proliferation in a mouse model of squamous cell carcinoma. Behav. Brain Funct. 10, 5.

Ye, Y., Dang, D., Zhang, J., Viet, C.T., Lam, D.K., Dolan, J.C., Gibbs, J.L., Schmidt, B.L., 2011. Nerve growth factor links oral cancer progression, pain, and cachexia. Mol. Canc. Therapeut. 10, 1667−1676.

Ye, Y., Ono, K., Bernabe, D.G., Viet, C.T., Pickering, V., Dolan, J.C., Hardt, M., Ford, A.P., Schmidt, B.L., 2014b. Adenosine triphosphate drives head and neck cancer pain through P2X2/3 heterotrimers. Acta Neuropathol. Commun. 2, 62.

Ye, Y., Scheff, N.N., Bernabe, D., Salvo, E., Ono, K., Liu, C., Veeramachaneni, R., Viet, C.T., Viet, D.T., Dolan, J.C., Schmidt, B.L., 2018. Anti-cancer and analgesic effects of resolvin D2 in oral squamous cell carcinoma. Neuropharmacology 139, 182−193.

Yeh, C.F., Li, W.Y., Chu, P.Y., Kao, S.Y., Chen, Y.W., Lee, T.L., Hsu, Y.B., Yang, C.C., Tai, S.K., 2016. Pretreatment pain predicts perineural invasion in oral squamous cell carcinoma: a prospective study. Oral Oncol. 61, 115−119.

Zhang, J.M., An, J., 2007. Cytokines, inflammation, and pain. Int. Anesthesiol. Clin. 45, 27−37.

Zhao, C.M., Hayakawa, Y., Kodama, Y., Muthupalani, S., Westphalen, C.B., Andersen, G.T., Flatberg, A., Johannessen, H., Friedman, R.A., Renz, B.W., Sandvik, A.K., Beisvag, V., Tomita, H., Hara, A., Quante, M., Li, Z., Gershon, M.D., Kaneko, K., Fox, J.G., Wang, T.C., Chen, D., 2014. Denervation suppresses gastric tumorigenesis. Sci. Transl. Med. 6, 250ra115.